

Cyclic growth of dermal papilla and regeneration of follicular mesenchymal components during feather cycling

Ping Wu¹, Ting-Xin Jiang¹, Mingxing Lei^{2,3}, Chih-Kuan Chen^{1,4}, Shu-Man Hsieh Li^{1,5,6}, Randall B. Widelitz¹ and Cheng-Ming Chuong^{1,*}

ABSTRACT

How dermis maintains tissue homeostasis in cyclic growth and wounding is a fundamental unsolved question. Here, we study how dermal components of feather follicles undergo physiological (molting) and plucking injury-induced regeneration in chickens. Proliferation analyses reveal quiescent, transient-amplifying (TA) and long-term label-retaining dermal cell (LRDC) states. During the growth phase, LRDCs are activated to make new dermal components with distinct cellular flows. Dermal TA cells, enriched in the proximal follicle, generate both peripheral pulp, which extends distally to expand the epithelial-mesenchymal interactive interface for barb patterning, and central pulp, which provides nutrition. Entering the resting phase, LRDCs, accompanying collar bulge epidermal label-retaining cells, descend to the apical dermal papilla. In the next cycle, these apical dermal papilla LRDCs are re-activated to become new pulp progenitor TA cells. In the growth phase, lower dermal sheath can generate dermal papilla and pulp. Transcriptome analyses identify marker genes and highlight molecular signaling associated with dermal specification. We compare the cyclic topological changes with those of the hair follicle, a convergently evolved follicle configuration. This work presents a model for analyzing homeostasis and tissue remodeling of mesenchymal progenitors.


KEY WORDS: Stem cell niche, Dermis, Follicle, Morphogenesis, Evolution, Evo-Devo, Chicken

INTRODUCTION

In adult animals, dermal mesenchymal components need to undergo physiological renewal for tissue regeneration and after injuries. These processes may occur via controlling residential mesenchymal progenitor stem cells (Brown et al., 2019; Nombela-Arrieta et al., 2011) or via reprogramming of differentiated cells (Knapp and Tanaka, 2012). How dermal mesenchymal cells renew themselves and maintain tissue homeostasis under physiological and wounding conditions is a fundamental question crucial to regenerative biology.

¹Department of Pathology, Keck School of Medicine, University of Southern California, Los Angeles, CA 90033, USA. ²111 Project Laboratory of Biomechanics and Tissue Repair, College of Bioengineering, Chongqing University, Chongqing 400044, China. ³Integrative Stem Cell Center, China Medical University Hospital, China Medical University, Taichung 40402, Taiwan. ⁴The IEGG and Animal Biotechnology Center, National Chung Hsing University, Taichung 402, Taiwan. ⁵Center for Craniofacial Molecular Biology, Ostrow School of Dentistry, University of Southern California, Los Angeles, CA 90033, USA. ⁶Department of Biochemistry, National Defense Medical Center, Taipei 114, Taiwan.

*Author for correspondence (cmchuong@usc.edu)

 P.W., 0000-0003-0035-8494; T.-X.J., 0000-0003-1972-8985; M.L., 0000-0002-4271-2714; C.-K.C., 0000-0002-0962-1589; S.-M.H., 0000-0001-7224-7094; R.B.W., 0000-0002-6603-4823; C.-M.C., 0000-0001-9673-3994

Handling Editor: Kenneth Poss
Received 15 November 2020; Accepted 8 July 2021

Both feather and hair follicles are discrete skin appendage units, with epidermal stem cell cycling (Chuong et al., 2013; Lai and Chuong, 2016). The control of hair follicle epidermal stem cell activation or quiescence has been well-characterized (Fuchs, 2018; Gonzales and Fuchs, 2017). Hair follicles contain two major dermal components, the dermal papilla (DP) and dermal sheath (DS) (Biernaskie, 2010). In the feather follicle, dermal components have a much more dominant presence. The mouse hair filament is an epidermal cord with multi-concentric layered keratinocytes induced above the DP, without dermal components invading into hair filaments (Gupta et al., 2019; Yang et al., 2017), whereas the developing feather filament has a dermal core within the epidermal cylinder.

Upon maturation, the cylinder opens up to become the two-dimension feather vane (Lucas and Stettenheim, 1972), with one side of the epithelium made of keratinized supra-basal cells, and the other side, originally the basal layer, facing the dermal pulp (Chuong et al., 2003). The epithelium of the whole feather filament is then covered by supra-basal cell-derived cuticles. The feather DP in the growth phase is large and gives rise to the abundant pulp that regenerates and degenerates cyclically in every feather cycle (Lillie and Wang, 1941; Lucas and Stettenheim, 1972). The feather cycle (Fig. S1A) enables the growth of different shaped feathers at different times during the life of the bird (Yu et al., 2004). During the growth phase, the epithelial long-term label-retaining cells are localized to the collar bulge region and are shown to be stem cells that generate feather structures (Yue et al., 2005). During the resting phase, these epithelial stem cells become quiescent and descend to the follicle base. The mature feather structure is then lost through molting. During the initiation phase of the next feather cycle, activation of these epithelial stem cells produces a new stem cell ring which gives rise to proliferative transit-amplifying (TA) cells, enabling feathers to elongate (Yue et al., 2005). This epidermal reactivation process requires the DP and is mediated by signals involving Wnt/DKK (Chu et al., 2014).

Although cyclic regeneration of feather epidermal components has been studied, the cyclic regeneration of dermal components has not. There are three types of dermal components in a growth-phase feather follicle: pulp (PP), DP and DS, adjacent to the feather follicle (Chen et al., 2015) (Fig. 1A', Fig. S1B-F). Loosely packed dermal pulp cells are located above the DP in the growth phase (Fig. 1A') and cell density differences can be observed between the peripheral and central parts of the pulp (pPP and cPP, respectively). Blood vessels within the pulp deliver nutrition to maintain feather follicle health (Lucas and Stettenheim, 1972) and may provide mechanical benefits to epidermal differentiation (Maderson et al., 2009). During avian feather regeneration, the feather epidermis grows continuously until it reaches the resting phase (Lucas and Stettenheim, 1972; Fig. 1B). The pulp grows along with the feather epidermis but maintains a nearly constant height after

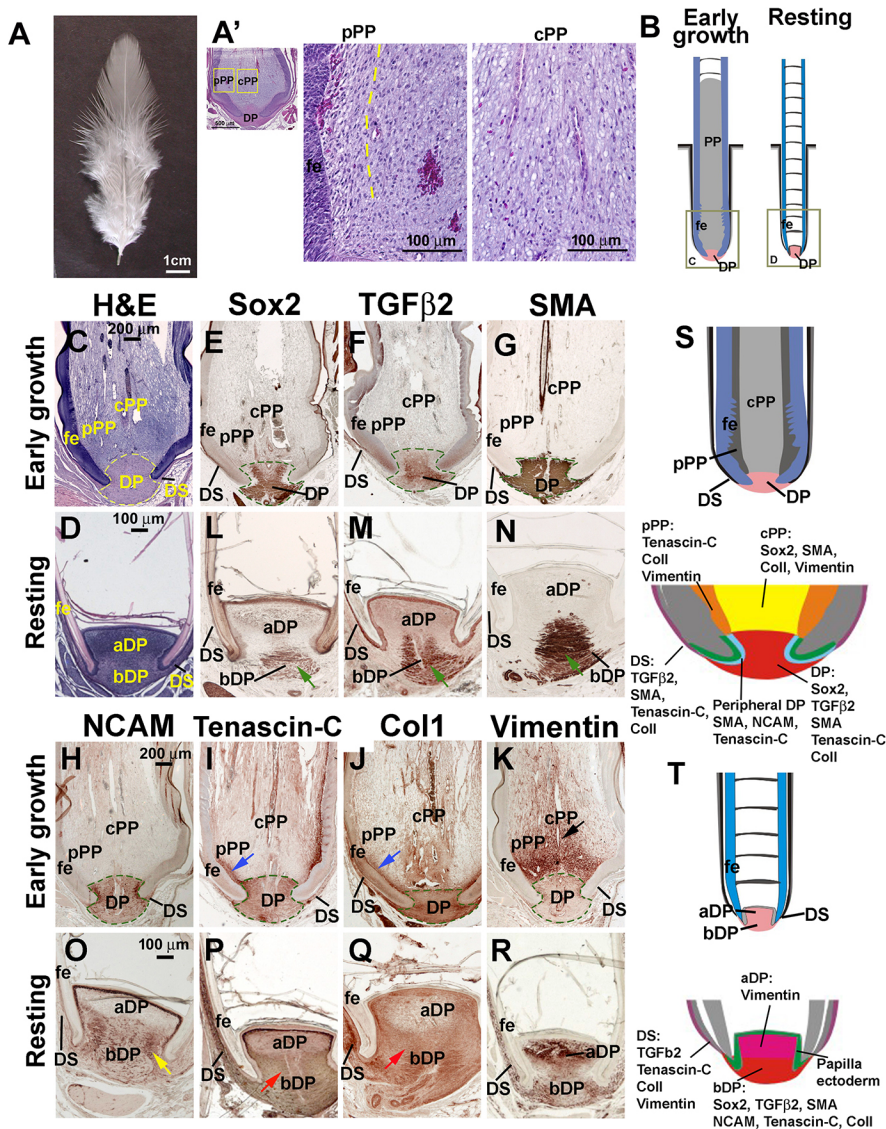


Fig. 1. Defining feather follicle-associated dermal components during feather cycling. (A) Brightfield view of a dorsal resting-phase contour feather from an adult male White Leghorn chicken. (A') H&E staining of a contour feather follicle in early growth phase showing the difference of pulp cell density between the area adjacent to the epidermis and the central part. The dotted line separates pPP and cPP. The thickness of pPP is 50-100 μ m, depending on the follicle size. Molecular marker can be seen in panels I, J. (B) Diagram of a contour feather follicle in growth and resting phases, respectively. (C-N) H&E staining (C, D) and immunostaining (E-R) of follicle at early growth phase (C, E-K), resting phase (D, L-R) showing Sox2 (E, L), TGF β 2 (F, M), SMA (G, N), NCAM (H, O), TNC (I, P), Col1 (J, Q) and vimentin (K, R). Blue arrows (I, J) indicate the pPP in early growth phase. Black arrow (K) indicates the cPP in early growth phase. Green arrows (L-N) indicate the positive signals in the resting-phase central bDP. Yellow arrow (O) indicates that NCAM is positive in the resting-phase bDP. Red arrows (P, Q) indicate that the staining is more positive in the resting-phase bDP. Dashed lines outline the DP. (S, T) Schematic summary of molecular expression in growth (S) and resting (T) phase feather follicles. aDP, apical dermal papilla; bDP, basal dermal papilla; cPP, central pulp; DP, dermal papilla; DS, dermal sheath; fe, feather epidermis; pPP, peripheral pulp.

\sim 2 weeks of regeneration. This is achieved by resorbing the distal pulp and forming pulp caps periodically. As the feather and sheath tissues continue to elongate, the apical pulp region becomes isolated from the lower dermal regions by epithelial pulp caps and the apical pulp degenerates (Lillie, 1940; Lucas and Stettenheim, 1972). The pulp diminishes at the end of feather regeneration, and apoptosis of the pulp epithelium allows the cylindrical feather filament epithelium to open up (Chang et al., 2004). Therefore, pulp undergoes regeneration, maintenance and degeneration processes in each feather cycle.

The topology of skin appendage follicles, allowing stem cells to be protected in the proximal follicle and the distal differentiated appendage to be shed, is a successful strategy for organizing the integuments (Lai and Chuong, 2016). Yet, the configurations of hair and feather follicles are achieved via convergent evolution, separated by \sim 200 million years. Although the fundamental principles of epidermal stem cells/dermal niche are shared (Chu et al., 2014; Fuchs, 2018; Morgan, 2014; Yue et al., 2005), the specific way to molt and regenerate the epidermal and dermal components during cycling are different. For example, the developing feather filament is a cylinder with pulp inside, whereas mouse and human hair filaments are concentric epithelial cords. To enter the resting phase,

feather follicles keep the follicular walls more or less intact, whereas hair follicles undergo catagen to destroy the lower follicles. Thus, it would be interesting to compare how these two major skin appendages, for avian and mammalian classes, may use different strategies to manage their cycling regeneration. In this study, we focus on dermal components. Recent work has provided considerable insight about the existence and identity of hair follicle dermal stem cells and how the DS, destroyed in catagen, is regenerated and cells in the DP are replenished (Chi et al., 2013; Rahmani et al., 2014; Shin et al., 2020). On the other hand, in feather cycling, there is much less remodeling of the DS, but very large-scale pulp regeneration and degeneration within the follicle. We wondered whether, in parallel to the epidermal cells in hair and feather follicles, there are also label-retaining cells (LRC), TA cells, stem cell clusters and progenitor cell zones in the dermis of growing feather follicles. If so, where are they located and how do they behave or transit during feather cycling?

Here, we use thymidine analog (BrdU, IdU and CldU) labeling to map dermal TA and LRC cells. We identified a pulp progenitor cell zone in the proximal collar region of the feather follicle, with LRC and TA cells. The LRC cell population position shifts dynamically through the physiological feather cycling. Using DiI to label the

lower DS cells in the growth phase, we found that DiI positive cells can give rise to cells in the DP and pulp. In addition, we use transcriptome analyses to identify key molecular expression. We track cellular flow and putative stem cells in feather dermal components throughout the feather cycle. We found marker genes in different feather dermal components and identified the molecular circuits regulating pulp growth and regeneration. This work represents a novel model for the study of homeotic control of dermal mesenchymal cell cycling under physiological regenerative processes.

RESULTS

Feather dermal components in growth and resting phases

A physiological feather cycle includes growth, resting and initiation phases (Yue et al., 2012). We observed that the growth phase of contour feathers in adult White Leghorn chickens lasted ~9 weeks in our housing conditions. Once the follicle reaches the resting phase (Fig. 1A), the feather stops growing and waits for signals to initiate the next cycle, which may occur physiologically or be induced by injury (e.g. plucking). We defined the different regenerating phases based upon the length of regenerated feathers in the central dorsal region (Fig. S1A, see Materials and Methods). Early growth- and resting-phase follicles display significant differences in their structures (Fig. 1B, schematic). Hematoxylin and eosin (H&E) staining shows that the early growth-phase follicle has the following dermal components: the DP, pPP, cPP, and DS. The DP and pPP, surrounded by feather epidermis (FE), have dense cellular packing, and the cPP are loosely packed with blood vessels (Fig. 1A',C; Fig. S1B). In contrast, pulp in the resting-phase follicle has degenerated and the epithelial parts are fully keratinized (Fig. 1B,D). In addition, the DP in the resting phase exhibits regional differences. The dorsal DP (or apical DP; aDP) has a higher cell density compared with the ventral DP (or basal DP; bDP). In both growth and resting phases, the DS locates beside the DP in the follicle sheath (Fig. 1C,D).

Immunostaining of extracellular matrix (ECM) and signaling molecules shows the heterogeneity of dermal components in a feather follicle (Fig. 1E-R). In the early growth phase, Sox2, TGF β 2, smooth muscle actin (SMA) and NCAM are expressed in the DP but not in the PP (Fig. 1E-H), whereas tenascin C (TNC), Coll1, and vimentin are expressed in both the DP and proximal PP (Fig. 1I-K). TNC and Coll1 are expressed in the entire DP and pPP (Fig. 1I,J, blue arrows). Vimentin is strongly expressed in the proximal PP (Fig. 1K, black arrow). In the resting phase, all these molecules show apical-basal differences. Sox2, TGF β 2 and SMA, which are positive in the early growth-phase DP, are expressed in the center of the basal DP in the resting phase (Fig. 1L-N, green arrows). NCAM is expressed in the lower two-thirds of the DP, with higher expression in the peripheral regions of the DP during the resting phase (Fig. 1O, yellow arrow), implying a concentric ring-like configuration in three dimensions. TNC and Coll1 are expressed in the entire DP with higher levels in the basal DP (Fig. 1P,Q, red arrows). Vimentin is more positive in the aDP (Fig. 1R). In the resting phase, the DP is seen to contain a molecularly distinct aDP and bDP. Thus, the growth-phase dermal components may include pPP, cPP, DP and DS, (Fig. 1S), whereas the resting-phase dermal components may include the aDP, bDP and DS (Fig. 1T). These data suggest that we can differentiate growth-phase pPP and cPP based upon: differences in cell density (Fig. 1A'), functional demonstration that they control barb branching patterns (Li et al., 2017) and pigmentation patterns (Lin et al., 2013), and molecular expression patterns (summarized in Fig. 1S).

The expression of diverse molecules suggests that a feather follicle has distinct dermal components with a dynamic status throughout different feather cycling phases (Fig. 1S,T). Interestingly, the molecular expression pattern indicates that resting-phase aDP shares similar expression profiles with growth-phase PP, whereas resting-phase bDP shares similar expression profiles with growth-phase DP, suggesting that resting-phase aDP may contain dermal progenitor cells used to regenerate the new pulp in the feather follicle following normal molting or plucking.

TA cells in the feather dermal components

To examine the TA cells in feather follicle-associated dermal components, we used short-term BrdU labeling (Fig. 2A). Two-hour BrdU labeling shows that the TA cell zone in the feather dermis is localized to the lower follicle pPP (Fig. 2B,C), close to the epidermis ramogenic zone. TA cells are also found sparsely distributed in cPP (Fig. 2C) but are rarely detected in the DP and DS during the growth phase (Fig. 2D).

We further performed continuous labeling of BrdU for 1 week and collected feather follicles without a chase period. Three stages of feather follicles (early growth, late growth and resting) were collected (Fig. S2). From the early growth- and late growth-phase samples, we confirmed that TA cell zones exist in the pPP during the growth phase (Fig. S2A,B, green arrows). In addition, we found that only a few BrdU-positive cells were detected in the DP and DS at all three stages (Fig. S2A'-C', pink arrows). This result demonstrates that the DP and DS in the growth and resting phases are in a latent state with a very low cell proliferation rate. The pPP is the only proliferation center in the feather dermal components, which may be crucial for feather growth.

To examine dynamic changes in pulp TA cells, we used a double-labeling method (Li et al., 2012) to mark proliferating cells with different thymidine analogs to observe cell proliferation and cell migration. We used CldU and IdU to label TA cells for 2 h and 24 h, respectively (Fig. 2E-I). We found that TA cell zones in both feather epidermis and pulp expanded with time (Fig. 2G). In the pulp, the TA cell zone expanded toward the cPP during the 24-h labeling period (Fig. 2G, second column), compared with the 2-h labeling period (Fig. 2G, first column). Compared with the pulp, the DP showed very few positive TA cells after both 2- and 24-h labeling periods (Fig. 2H, first and second column). We calculated the percentage of 2-h labeled CldU cells versus 24-h labeled IdU cells in pPP and cPP and showed that the percentage of TA cells increases more in the cPP than in the pPP (Fig. 2I,J). This double TA cell labeling result demonstrates the migration and expansion of pulp cells and illustrates their possible migration route (Fig. 2K).

Long-term label-retaining dermal cells in the feather dermal components

The distribution of putative feather dermal stem cells at different regeneration stages were assessed using long-term labeling followed by a chase period (Fig. 3A,B). In brief, chickens with contour feathers that regenerated for 1 week were labeled with BrdU for 1 week then chased for 2-7 weeks (Fig. 3B). We collected feather follicles at different weeks during regeneration, which correspond to early growth, middle growth, late growth and resting phases, respectively (Fig. 3A).

After 1-week labeling, 90.2 \pm 4.1% (mean \pm s.d.) of the pPP cells are BrdU positive (Fig. 3C,C', yellow arrows), but the DP and the DS are rarely positive. After a 2-week chase, the number of BrdU-positive cells in the pPP decreased to 31.5 \pm 5.1%. These BrdU long-term label-retaining dermal cells (LRDCs) are concentrated in the

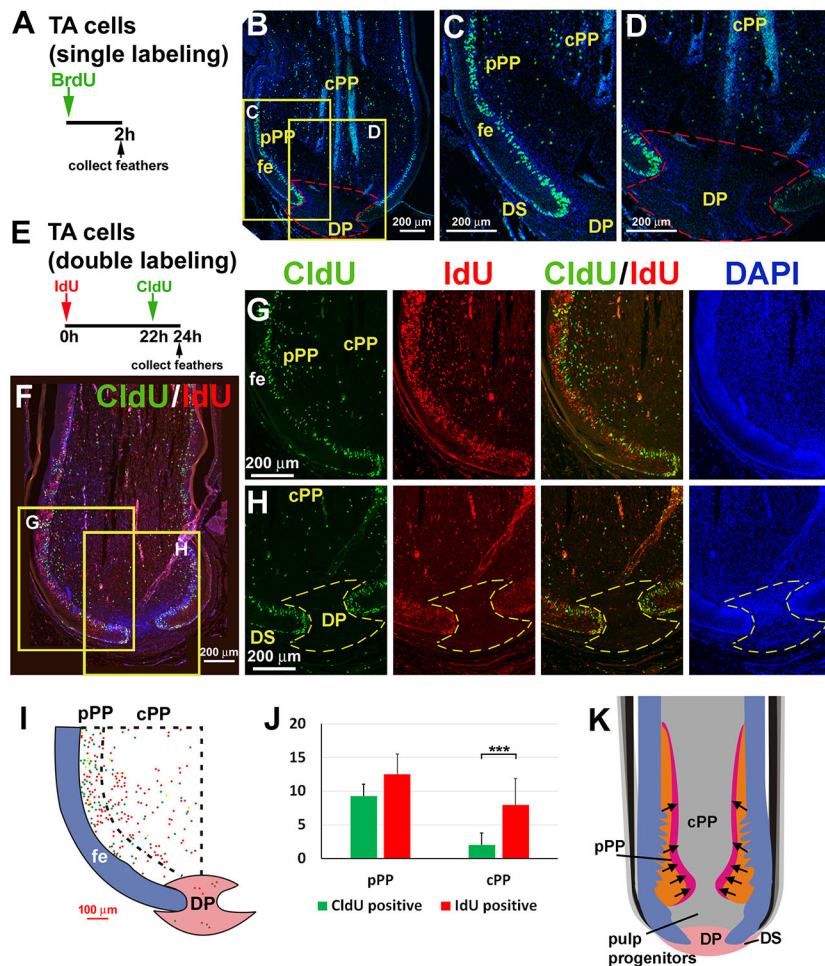


Fig. 2. The behavior of TA dermal cells during feather cycling. (A) Strategy of pulse BrdU TA cell labeling. (B) BrdU staining of an early growth-phase contour feather follicle. (C, D) Higher magnification of PP (C) and DP (D) regions (yellow boxed areas in B). (E) Strategy of double TA cell labeling. The thymidine analogs IdU and CldU are injected at different time points. (F) Double staining of an early growth-phase follicle labeled with CldU for 2 h (green) and IdU for 24 h (red), respectively. (G, H) Higher magnification views of the pulp (G) and DP (H) regions (yellow boxed areas in F). First column, 2-h CldU labeling; second column, 24-h IdU labeling; third column, combined; fourth column, DAPI staining. Red streaks in the cPP region are blood vessels. (I) Diagram showing CldU-positive (green dots) and IdU-positive (red dots) cells. Dotted line separates the pPP from the cPP. The percentages of CldU- and IdU-positive cells were calculated ($n=5$ feather follicles, $***P<0.001$, paired two-tailed Student's *t*-test). (J) Percentage of CldU- and IdU-positive cells in pPP versus cPP. Data are mean \pm s.d. (K) Schematic summary showing the dermal TA cell population and potential migration trend in early growth-phase follicles. Black arrows indicate the dermal cell migration route in PP. Dashed lines in B, D and H outline the DP. cPP, central pulp; DP, dermal papilla; DS, dermal sheath; fe, feather epidermis; pPP, peripheral pulp.

pPP, adjacent to the epidermal LRC in the collar bulge, previously shown to be the site of feather epidermal stem cells (Fig. 3D, D', white arrows). Some LRDCs can also be detected in the DS (Fig. 3D, green arrows). Feathers collected after a 4-week chase period showed that the LRDCs moved downward surrounding the DP (Fig. 3E, E', white arrows) and some DS cells are BrdU positive (Fig. 3F, green arrows). Notably, downward movement of putative dermal stem cells accompanies the movement of the epidermal stem cell zone (yellow bracket line in Fig. 3D, E). After a 7-week chase period, the resting-phase feather follicle has LRDCs in the aDP (Fig. 3F, F', blue arrows) and some positive cells also are seen in the DS (Fig. 3F, F', green arrows). The schematic drawings (C'-F') show the relative position of BrdU-positive cells (blue dots, no chase; yellow dots, LRCs in epidermis; red dots, LRDCs in dermis). The percentage of BrdU-positive cells before and after 2-, 4- and 7-week chase periods are shown in Fig. 3G. These results demonstrate that the accompanied downward shift of epidermal and dermal LRCs during feather cycling (Fig. 3H). In the resting phase, LRDCs are present in the aDP but not in the bDP, suggesting that the aDP region may retain dermal progenitor cells for the next feather cycle. The bDP is more quiescent than the aDP.

We co-stained the LRDCs and the marker genes shown in Fig. 1. Examples (*Coll*, *TNC* and *Sox2*) are shown in Fig. S3. The distribution of LRDCs in different developing stages are accompanied with the differential expression of marker genes. For example, when LRDCs move downward from middle growth to late growth and eventually present in the aDP in resting phase

(Fig. S3C, F, I), the expression of Sox2 antigen changed from the whole DP (middle growth and late growth) to the bDP (resting phase).

Molecular profiling of pulp in different feather cycle stages

We investigated the transcriptomes of the cycling pulp. We collected early growth-phase, late growth-phase and near resting-phase feathers (Fig. 4A). Pulp was dissected out. Resting-phase DPs were also collected and separated into aDP and bDP. We performed RNA-seq and compared the RNA expression profile at different feather developmental stages, e.g. from early growth-PP to late growth-PP to near resting-PP to resting-phase aDP, then back to early growth-PP (Fig. 4B, C). We identified the differentially expressed genes (DEGs) in each developmental phase and visualized their expression profiles using a heatmap with hierarchical clustering (Fig. 4C; Tables S1, S2). The lowest number of DEGs is in the transition from late growth phase to near-resting phase (491 upregulated and 148 downregulated); whereas the highest number of DEGs is found between the resting-phase aDP and early growth-phase PP (1299 upregulated and 1048 downregulated) (Table S1). This result suggests new feather initiation needs activation of many molecular pathways to promote pulp growth.

Further examination of gene expression levels among different developmental stages reveals that *CDK1*, *SOSTDC1*, *WNT2b* and *WNT11* were decreased in the PP from the early growth to late growth phases, whereas the Wnt antagonist *WIF1* was increased in the same time interval (Fig. 4D). *In situ* hybridization of

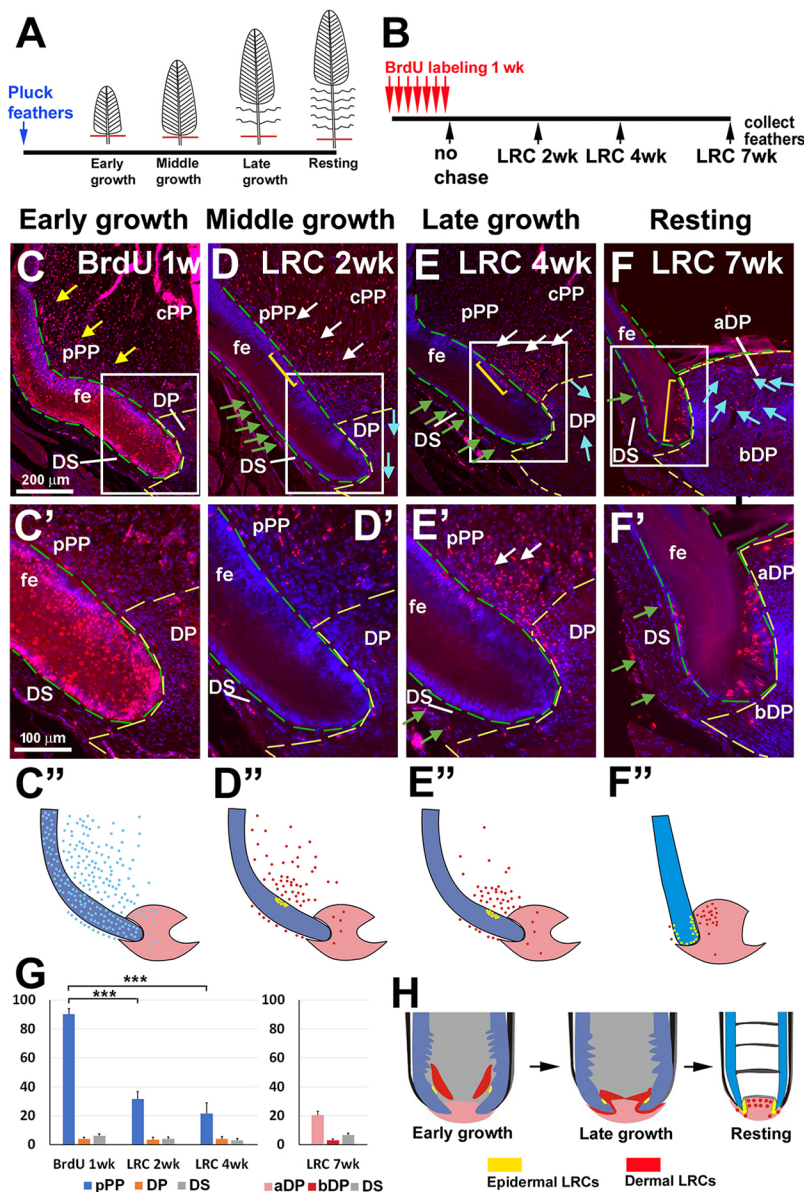


Fig. 3. The behavior of long-term label-retaining dermal cells during feather cycling. (A) Contour feathers are plucked and allowed to regenerate. (B) Strategy to identify LRCs. BrdU labeling begins 1 week after contour feather regeneration. Chickens are labeled with BrdU for 1 week. Feathers are collected at time points representing different cycle stages. (C) A feather follicle labeled with BrdU for 1 week without chasing. (D-F) Feather follicles are chased for 2 (D), 4 (E) and 7 (F) weeks. Collected feathers are in the middle growth, late growth and resting phase, respectively. Green dashed line outlines the feather epidermis. Yellow dashed line surrounds the DP. Yellow arrows (C) indicate the BrdU-positive cells in PP after 1-week labeling. White arrows (D,E) indicate the LRCs in PP. Green arrows (D-F) indicate LRCs in the DS. Blue arrows (D-F) indicate LRCs in the DP. Note the LRCs accumulate in the aDP in resting phase (F). Yellow brackets (D-F) indicate the epidermal stem cells. (C'-F') Higher magnification images of boxed areas in C-F. (C''-F'') Schematic showing the relative position of BrdU-positive cells (blue dots, no chase; yellow dots, epidermal LRCs; red dots, dermal LRCs). (G) Left: percentage of BrdU-positive cells before and after a 2- and 4-week chase period in the pPP, DP and DS. Right: percentage of BrdU-positive cells after a 7-week chase period in the aDP, bDP and DS. For each time point, $n=5$ follicles, $***P<0.001$ (paired two-tailed Student's *t*-test). Data are mean \pm s.d. (H) Diagram of LRCs in early growth, late growth- and resting-phase feather follicles. Yellow represents stem cells in the feather epidermis. Red indicates putative dermal stem cells in feather follicles at different regeneration stages. aDP, apical dermal papilla; bDP, basal dermal papilla; cPP, central pulp; DP, dermal papilla; DS, dermal sheath; fe, feather epidermis; pPP, peripheral pulp.

CDK1 (Fig. 4F) and *SOSTDC1* (Fig. 4H) showed that their expression distribution and levels decreased as feather development progressed. ECM molecules demonstrated fluctuations in expression of *NCAM* and collagens *COL13A1* and *COL23A1* (Fig. 4E). *MMP9* expression increased and peaked at near resting phase, when the pulp shrinks down to become the future aDP (Fig. 4E). *MMP* gene family members are involved in ECM breakdown during normal physiological processes, such as embryonic development, reproduction and tissue remodeling (Assis-Ribas et al., 2018). Fluctuating ECM and *MMP9* expression levels suggest that they may play important roles in feather cycling. We further performed a double-immunostaining of *COL2A1* (red) and *MMP9* (green) at different feather cycle stages (Fig. 4G; enlarged views of the boxed areas are shown in the lower panels and the separated channels are shown in Fig. S4). The results demonstrate the dynamic expression domains of *COL2A1* and *MMP9* at different feather cycle stages. *COL2A1* and *MMP9* expression patterns are similar but not identical in the late growth and near resting phases. Both genes are expressed in the pulp close to the DP, although *MMP9* is expressed in a

narrower domain (Fig. 4G, second and third column). Both *COL2A1* and *MMP9* expression levels decreased in the resting phase (Fig. 4G, fourth column). This result suggests that *MMP9* may play a crucial role in remodeling pulp tissue during feather cycling.

Molecular profiling in different dermal components

We wondered what key genes are expressed in different dermal components and whether they may provide clues to cell fate specification in the regenerating feather follicle. To identify the molecular expression of different dermal components, we performed RNA-seq focusing on the early growth-phase feather follicle. Four dermal components, including the cPP, pPP, DP and DS were dissected. Triplicate biological RNA libraries were prepared and sequenced for each component (Fig. 5A). Principal component analysis (PCA) revealed that replicate samples clustered closer to each other than to other samples from other dermal components (Fig. 5B). We then performed pairwise comparisons between all the libraries and acquired 1860 unique DEGs (Fig. 5C; Table S3). Hierarchical clustering and heatmaps from the unique

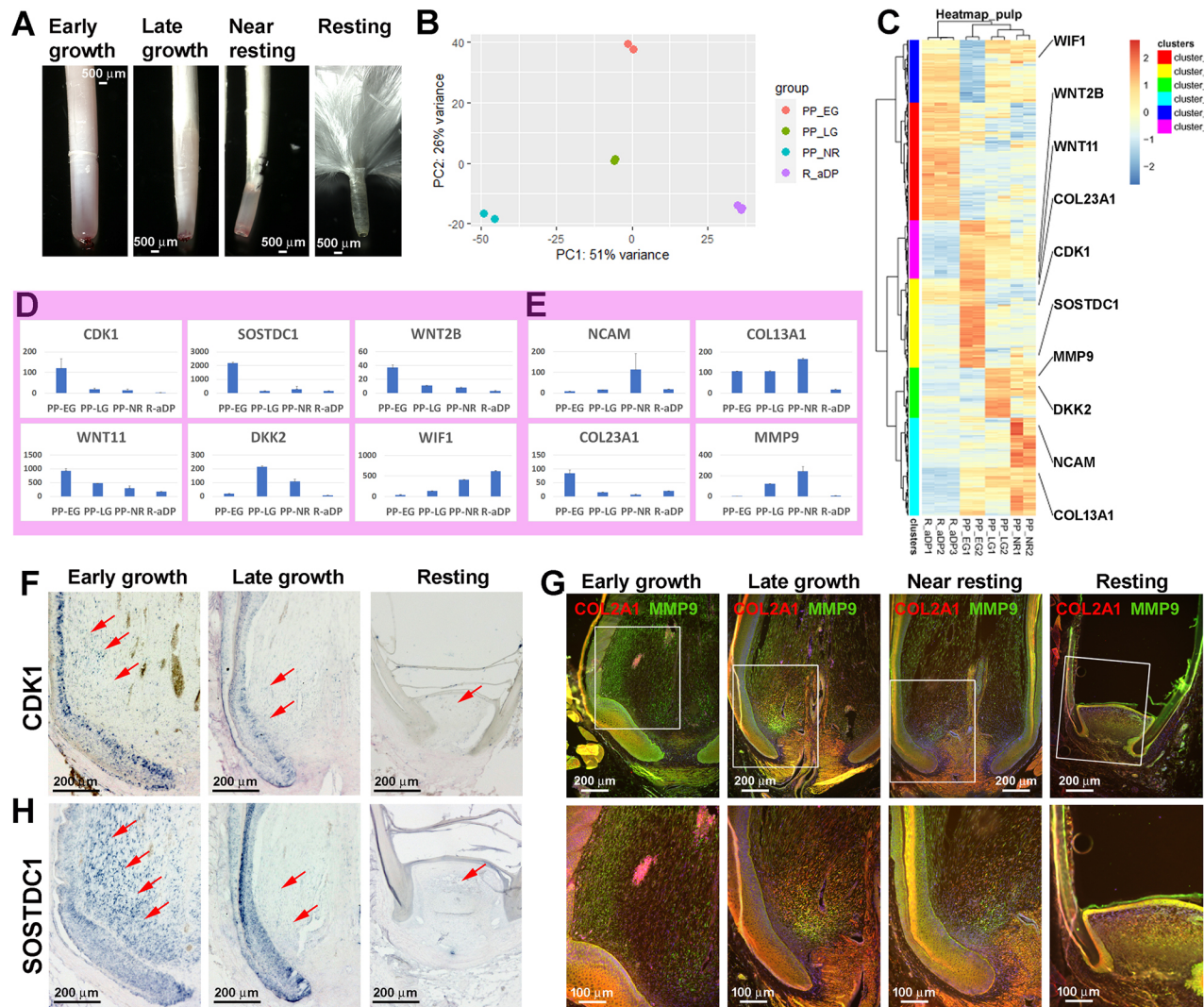


Fig. 4. Dynamic molecular expression in dermal components during feather cycling. (A) Brightfield view of the plucked proximal feather follicle at different regeneration phases. (B) PCA analysis of RNA-seq showing the pulp at different growth phases and during the resting-phase aDP. (C) DEG clustering analysis and the expression heat map. (D,E) Expression level of signaling molecules (D) and ECM (E) in different pulp formation stages. Data are mean \pm s.d. (F,H) *In situ* hybridization of *CDK1* (F) and *SOSTDC1* (H) in different pulp developmental stages. Red arrows indicate the expression in pPP (growth phase) and aDP (resting phase). (G) Immunostaining of COL2A1 (red) and MMP9 (green) in different pulp developmental stages. Boxed areas are shown enlarged in the lower panels. The separated green and red channels are shown in Fig. S4. aDP, apical dermal papilla; bDP, basal dermal papilla; cPP, central pulp; DP, dermal papilla; DS, dermal sheath; EG, early growth phase; LG, late growth phase; NR, near resting phase; pPP, peripheral pulp.

DEGs show marker genes exclusively upregulated in each dermal component (Fig. 5D). Accordingly, genes in clusters 2+6, clusters 10+1, cluster 5 and cluster 4 were defined as markers of the DP, DS, pPP and cPP, respectively (Table S4).

Examples of expression profiling from each dermal component are shown in Fig. 5E. *CRABP-1*, *LGR5* and *COL13A1* are highly expressed in pPP, whereas *MMP9*, *SOSTDC1* and *COL23A1* are highly expressed in cPP. Note that *COL13A1* and *COL23A1* are expressed in both pPP and cPP. For DP, we show that *NCAM*, *BMP4* and *NOG2* are highly expressed. *FZD8*, *COL28A1* and *TGFB2* are highly expressed in DS.

We further performed RNAscope to find the expression of *FZD8*, *TNC* and *NCAM* in the same section of a growth-phase feather follicle. *FZD8* transcripts are located in the lower DS and epidermal cells close to the DP (Fig. 5F). *TNC* mRNA is found in the DP, lower DS and pPP (Fig. 5G), whereas *NCAM* is enriched in the DP

and DS (Fig. 5H). The merged expression of these three molecules is shown in Fig. 5I. Furthermore, we examined whether dermal LRDCs co-express the molecules enriched in dermal components. We used RNAscope to detect *TNC* and *NCAM* transcripts in the near resting-phase feather follicle and co-stained the LRDCs in the same section (Fig. S5). We focused on the distribution of dermal LRDCs in pPP and DS. We found the accumulation of LRDCs in the pPP (Fig. S5G) was accompanied by higher *NCAM* expression levels (Fig. S5H). In the DS, fewer LRDCs were detected (Fig. S5L) and both *NCAM* and *TNC* were expressed at lower levels than in the pPP (Fig. S5M,N). Based on this data, we speculate that the higher expression levels of cell adhesion molecules, such as *NCAM*, in the near resting-phase PP (Fig. 4E) may be involved for the accumulation of LRDCs required for feather cycling. Further study will be required to characterize these LRDCs and the DS in the future. In this study, we focused more on the regeneration of feather pulp.

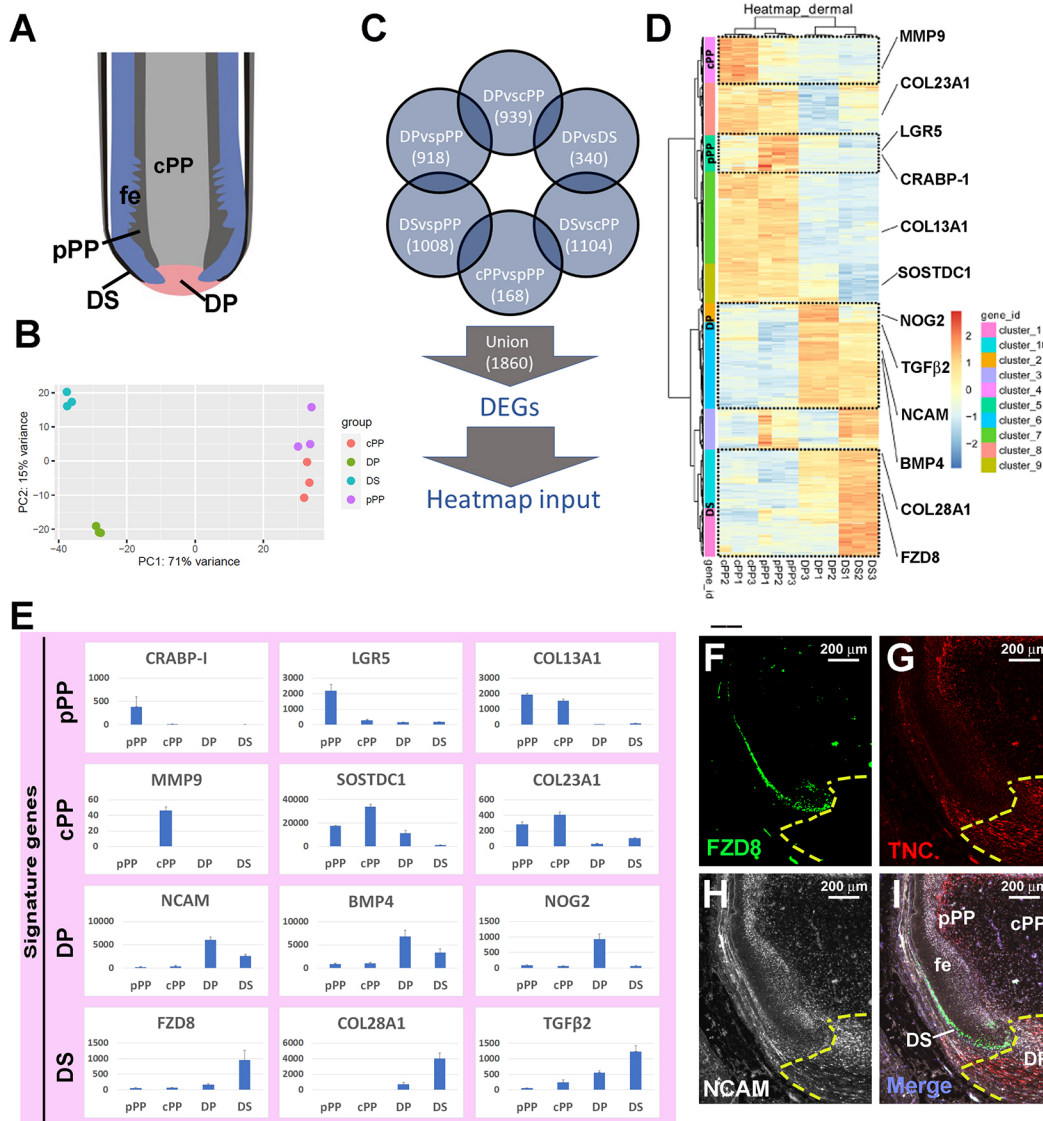


Fig. 5. Transcriptome analyses highlight key genes associated with the activation of dermal components in early growth-phase during feather cycling. (A) Diagram shows different dermal components in an early growth-phase feather follicle. (B) PCA analysis of four dermal components. (C) Strategy of finding marker genes in different dermal components. (D) DEG clustering analysis and the expression heat map. Clusters with marker genes are highlighted by dashed squares. (E) Marker gene expression levels in different dermal components. Data are mean \pm s.d. (F-I) Expression of FZD8 (F), TNC (G) and NCAM (H) in early growth-phase feather follicles revealed by RNAscope. (I) Merged images. Dotted lines in F-I outline the DP. cPP, central pulp; DP, dermal papilla; DS, dermal sheath; fe, feather epidermis; pPP, peripheral pulp.

LRDCs in DP contribute to feather pulp regeneration

Resting-phase DP retains LRDCs in the apical region (Fig. 3F). We wondered whether these LRDCs contribute to feather regeneration after plucking. Therefore, we plucked resting-phase feathers, then we collected feather follicles at 0 (immediately after feather removal), 2 and 4 days (Fig. 6A). H&E staining of these follicles showed that the aDP gives rise to new pulp 2 days after regeneration starts (Fig. 6B, middle panel). The size of the pulp continues to expand at 4 days after regeneration (Fig. 6B, right panel). The regeneration is accompanied by higher K15 and Lgr6 expression in the feather epidermis and follicle sheath (Fig. 6C,D). To examine whether the LRDCs in the aDP participate in new PP formation, we used IdU to label the LRDCs in the growth phase. After feathers entered the resting phase, they were plucked and allowed to regenerate for 2 days. Two hours before collecting the follicle, we injected CldU to label the TA cells. The regenerated feather follicles

were then collected and the distribution of both dermal LRCs and TA cells was determined (Fig. 6E). In normal resting-phase feathers, LRDCs were located in the aDP (Fig. 6F). Two days after plucking induced regeneration, we detected numerous TA cells in the epidermis and new PP (Fig. 6G, red dots). We also detected some LRDCs in the new PP (Fig. 6G, blue dots). To test whether LRDCs in the resting-phase aDP become TA cells in the regeneration process, we used fluorescent immunostaining to detect LRDCs (red) and TA cells (green) (Fig. 6H). We found that among IdU-positive cells, 53.3 \pm 9.9% were also CldU positive (Fig. 6H, white arrows). Quantification of the percentage of IdU-positive cells (LRCs), CldU-positive cells (TA cells) and double-labeled IdU/CldU-positive cells are shown in Fig. 6I. This result demonstrates that 53.3% of LRDCs in the aDP became TA cells, suggesting the important role of aDP as putative dermal stem cells in feather regeneration (Fig. 6J).

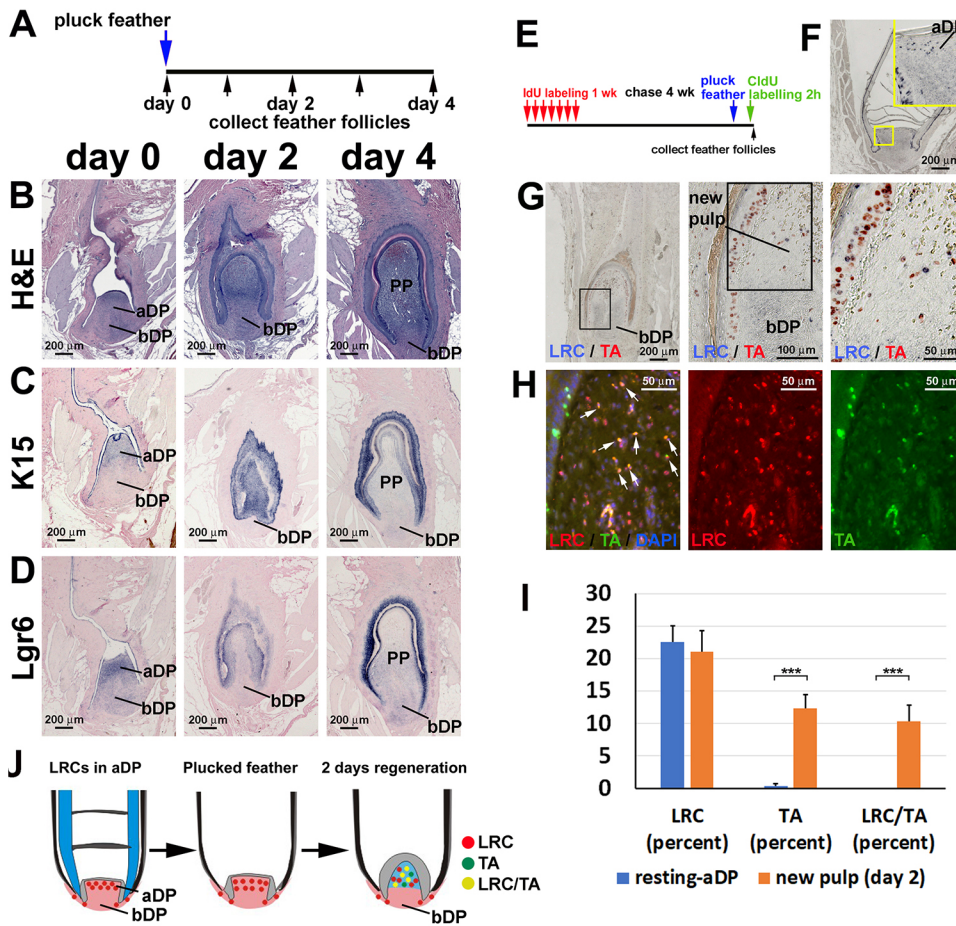


Fig. 6. Long-term label-retaining dermal cells in the apical dermal papilla contribute to pulp regeneration.

(A) Strategy to collect regenerating feather follicles at different time points. (B) H&E staining of feather follicles. (C, D) *K15* (C) and *Lgr6* (D) *in situ* hybridization. (B–D) Left column, feather follicles after plucking at resting phase; middle column, 2 days after plucking; right column, 4 days after plucking. (E) Strategy of LRDCs and TA cell double labeling with IdU and CldU, respectively. (F) IdU staining of a resting-phase feather follicle showing the LRCs in the aDP. (G) Double staining of LRDCs (blue) and TA cells (red) in a follicle regenerating for 2 days. (H) Fluorescent immunostaining of LRDCs (red) and TA cells (green). White arrows indicate the double-labeled new PP cells. (I) Percentage of CldU-positive cells (TA cells), IdU-positive cells (LRCs), and double labeled CldU/IdU-positive cells in the resting-phase aDP and new pulp after 2 days of regeneration ($n=4$ feather follicles, $***P<0.001$, paired two-tailed Student's *t*-test). Data are mean \pm s.d. (J) Schematic showing LRDCs in aDP participating in pulp regeneration. aDP, apical dermal papilla; bDP, basal dermal papilla; PP, pulp.

Tracking dermal cellular flows in feather follicles

To trace the dermal cell lineage within the feather follicle, we used different methods to label the DP and DS. We used DiI to label the DP cells. To do this, the early growth follicle sheath was opened and DiI solution was micro-injected in the dorsal part of the DP (Fig. 7A). We found that the dorsal pPP is DiI positive ($n=5$), suggesting that some DP cells move upward to form the pulp. To label the DP cells in the resting phase, we plucked resting-phase feathers and opened their follicle walls. DiI was injected into the dorsal aDP. After 5 days, the feather follicles ($n=5$) were dissected and we found that some DiI-positive aDP cells become pulp cells (Fig. 7B).

We further used DiI to label lower DS cells in the growth phase ($n=4$) without plucking. After 24 h, we found that some pPP cells had a red signal, suggesting that these cells migrated from the DS (Fig. 7C, red arrows). In addition, we used a Tol2 labeling method to label lower DS. To do this, pT2AL200R175-CAGGS-H2BGFP/pCAGGS-T2TP plasmids were injected into lower DS and electroporation was performed (Fig. 7D). Samples were collected after 48 h and frozen sections were prepared (Fig. 7D, second column, brightview). We found positive H2BGFP signals in the pPP, about 2 mm above the DP (Fig. 7D, green arrows).

These results suggest that some lower DS cells can generate pPP cells. Although we do not have the genetic lineage-tracing method used in the transgenic mouse system, these different strategies show the overall trend that dermal cells flow dynamically from the lower DS to DP and PP. Whether there are dermal cup-like cells in the lower DS of feather follicles remains to be defined. Experimental methods in the chicken are still being developed for higher-resolution lineage tracing.

DISCUSSION

Feather follicle-associated dermal population is organized as quiescent stem cells, activated progenitors, TA cells and differentiated cells

In this study, we show a mesenchyme cycling model in which multiple dermal components in a discrete follicle unit undergo cyclic physiological regeneration. Some of the multiple complex dermal components serve as a dermal niche for epidermal and melanocyte patterning morphogenesis, some differentiate to become nutrient providing pulp and some are reserved as quiescent dermal stem cells for the next feather cycle. Here, we have analyzed the homeotic control of these dermal populations. We located the TA cells and LRDCs in different feather dermal components and observed that, in the growth phase, dermal LRCs are in the pPP adjacent to epidermal LRCs in the collar bulge. As feathers enter the resting phase, dermal LRCs gradually move down to the aDP (Fig. 3H). In the next cycle, the aDP then generate new pulp cells, as LRDCs proliferate to participate in this regeneration process (Fig. 6J). Based on our results, we speculate that the bDP may be the site of quiescent DP stem cells, whereas the aDP represents activated DP stem cells, although higher resolution experiments need to be carried out when techniques become available. Here, we propose our current understanding of the logic of feather dermal component cycling during physiological feather follicle cycling (Figs 7E and 8). It is most interesting that similar LRC, TA and differentiated populations controlling hair/feather epidermal cells are found in parallel in these dermal cells. Furthermore, dermal and epidermal LRCs co-migrate during feather cycling, suggesting some shared molecular control. Yet the

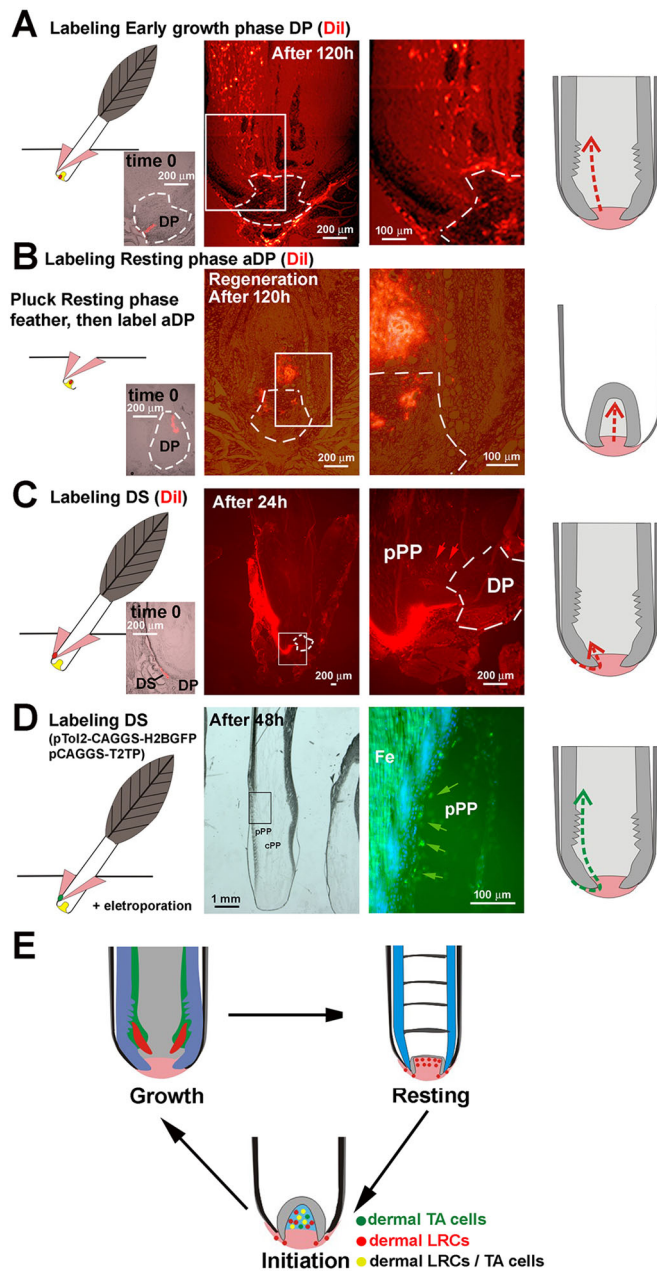


Fig. 7. Tracking dermal cells in feather follicle. (A–D) Tracking dermal cellular flow in growth-phase feather follicle. Dil labeling of early growth-phase DP (A), resting-phase DP (B), early growth-phase DS (C) and labeling DS using the Tol2 system (D). Left column, schematic showing the labeling position. Pink shows the opened follicle sheath surrounding the feather follicle. Yellow and green indicate the injection site. Insets show the follicles immediately after Dil labeling. Second and third columns, fluorescent signals after indicated time intervals. Right column, schematic summarizing cell lineage tracing results. (E) Homeostasis of LRDCs and TA cells during feather cycling. DP, dermal papilla; DS; dermal sheath; pPP; peripheral pulp.

molecular modules controlling these behaviors remain to be investigated.

Comparing the dynamic topology of the dermal components in mouse hairs and chicken feathers, two convergently evolved skin appendage follicles

One motivation for this study was to find how hair and feather follicles evolved with similarities and differences during their

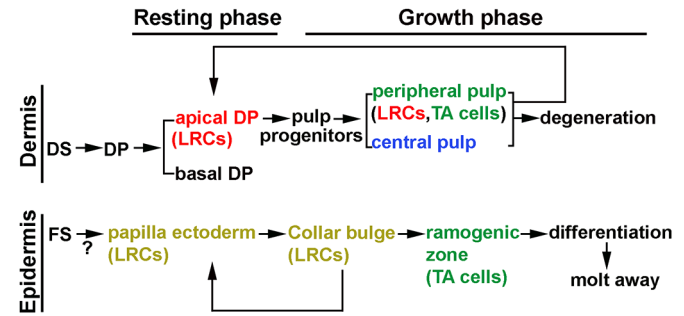


Fig. 8. Comparison of dermal components between hair and feather follicles. Cycling of follicle components during feather cycling. DP, dermal papilla; DS; dermal sheath; FS, follicle sheath; LRC; label-retaining cells; TA, transient amplifying cells.

~200 million-years of independent evolution. The results are summarized in Table 1. In hair follicles, the DP serves as the signaling center to regulate hair growth and regeneration (Morgan, 2014). The DP size and cell numbers fluctuate during hair cycling, suggesting that hair follicle mesenchymal components have significant hair cycle-associated plasticity (Tobin et al., 2003). The cell proliferation rate is low in the hair DP (Elliott et al., 1999). The DS cells can also regenerate a new DP upon grafting to a host (Horne and Jahoda, 1992; McElwee et al., 2003) via the PI3K-Akt pathway (Feutz et al., 2008). The adult DS harbors dermal stem cells, which regenerate a new DS and supply cells to the DP (Biernaskie, 2010). Using *in vivo* lineage tracing and *in vitro* clonal analysis, it is shown that the adult DS harbors dermal stem cells, which repopulate the DS and the DP with new cells (Rahmani et al., 2014). Hair follicle dermal stem cells can regenerate the DS and repopulate the DP (Chi et al., 2010; Rahmani et al., 2014). Platelet-derived growth factor (*Pdgfra*) signaling is important for the function of hair follicle dermal stem cells (González et al., 2017). The hair DS has a distinct precursor population which may act as a reservoir for regenerating DP cells in aging (Agabalyan et al., 2017). Injury of hair follicles was shown to recruit more dermal stem cell progeny to become DP cells (Abbasi and Biernaskie, 2019).

In feather follicles, previous transplantation studies have shown that the DP controls epidermal stem cell fate, implying different branch forms can be modulated based on molecular signals (Yue et al., 2005). Rachis formation results from an anterior-posterior *Wnt3a* gradient that tilts the radially symmetric barb ridges to generate a rachial ridge (Yue et al., 2006). Retroviral-mediated ectopic fibroblast growth factor 10 (*FGF10*) expression produced short and broad feathers, especially in the proximal regions. Ectopic expression of *Sprouty 4* (*SPRY4*), an *FGF* antagonist, induced distal branched structures to form abnormally in the proximal feather sheath (Yue et al., 2012). This cycling process fine-tunes *Wnt* signaling to control feather regeneration and axis formation (Chu et al., 2014).

We have compared the morphological/structural similarities and differences between chicken feathers and mouse hairs (Table 1). In mouse hair cycling, the lower hair follicle is destroyed in catagen. In every anagen, DS is regenerated along with outer root sheath (ORS) and hair matrix. Thus, the regeneration of dermal components is mainly DS and some DP, with cells coming from the dermal cup, the location of dermal stem cells (Rahmani et al., 2014). In contrast, in feather cycling the major degeneration events occur in the pulp and epidermal collar within the follicle. Thus, the major feather dermal components that require regeneration are the pulp and some DP, not DS. In feather follicles, in addition to the inductive function of DP

Table 1. Similarity and difference of dermal components between hair and feather follicles

	Mouse hair	Feather
Dermal components	DP, DS	DP, DS, pulp
Dermal pulp	None	Central pulp: nutrition (Lucas and Stettenheim, 1972); Peripheral pulp: interacts with epidermis (Lin et al., 2013; Li et al., 2017) Undergoes cyclic degeneration and growth
Dermal papilla		
Cell proliferation	Rarely	Growth phase, rarely; resting phase, quiescent; initiation, apical part is active to generate pulp progenitors which give rise to peripheral and central pulp
Cell number	Fluctuates during cycling (Chi et al., 2013)	Fluctuates, pulp shrinks and descends to become the apical DP in resting phase
Heterogeneity	Four major subpopulations in the anagen DP (Yang et al., 2017)	Growth phase, mainly in the basal DP; resting phase, in both the apical and basal DP
Dermal sheath		
Dermal cup and lower dermal sheath	Harbors dermal stem cells which regenerate a new dermal sheath and repopulates cells into the DP during hair cycling (Rahmani et al., 2014)	Some LRDCs are detected in the lower DS; labeled lower DS cells can give rise to the DP and pulp cells. Whether there is an equivalent cell population as seen in the hair dermal cup remains to be determined
Upper dermal sheath	Undergoes cyclic degeneration in catagen and regeneration in anagen	Maintains similar height from the follicular base to follicular orifice

DP, dermal papilla; DS, dermal sheath; LRDC, long-term label-retaining dermal cell.

(Chu et al., 2014), the cPP in the filament core provides nutrition continuously for feather growth. Furthermore, an additional pPP-epidermal interface is extended distally above the DP (discussed further in the next section). Feather DS, DP and PP are contiguous structures. When feathers enter the resting phase, no pulp component remains and LRDCs descend to reside in the aDP. Because the dermal components that require regeneration are differently positioned in hair and feather follicles, the topological arrangement of dermal LRDCs and TA cells are also different. Whether there is a parallel dermal cup equivalent in the lower sheath remains to be studied using transgenic chickens in future investigations.

Cyclically regenerated feather dermis enables the highly modifiable stem cell niche and complex feather architectures to be built along the proximal-distal axis of the feather shaft

What is the biological implication of this extensive remodeling dermal niche in feather follicles? The structure of the feather follicle forms a proximal-distal growth gradient. The older, more-differentiated cells involved in branching morphogenesis localize toward the distal end (Chen et al., 2015). The immature epithelial cells localize in the proximal end of the follicle and surround dermal components. Studies have shown that feather structures are formed and maintained by a balance of different growth factor activities at the specific time epidermal stem cells undergo branching morphogenesis. For example, the anterior-posterior *Wnt2b* gradient in the contour feather DP leads to different feather branching phenotypes, leading to the co-linear formation of pennaceous vanes or plumulaceous branches along the distal-proximal axis of the feather shaft (Chang et al., 2019).

The extension of the pPP layer, adjacent to the epidermal progenitor cells in the collar region, is extended from the DP toward the distal ramogenic zone. This remarkable feature allows prolonged interactions between the dermal niche and epidermal stem cells, providing a tunable interface. This dermal layer contains signaling molecules to affect epidermal morphogenesis and pigment patterning (Li et al., 2017; Lin et al., 2013). Formation of the pPP is an evolutionarily novel feature that allows for fine-tuning of signaling modules to build more complex feather architectures, with temporal changes of dermal niche activities projected on to the spatial distal-proximal feather axis.

Our bulk RNA-seq for pulp at different developing phases (Fig. 4) and in different dermal components (Fig. 5) suggest the possible molecular circuit regulating cell proliferation and migration in feather growth. For example, decreasing *CDK1* expression from early growth PP to resting-phase aDP (Fig. 4D,F) is accompanied by the declining number of BrdU-positive cells (Fig. S2). *NCAM* is another molecule which showed an intriguing pattern. *NCAM* transcripts are found at higher levels in the DP and DS (Fig. 5E), whereas RNAscope results reveal the heterogeneous *NCAM* transcript distribution in the DP: the peripheral DP expresses higher *NCAM* levels than the central DP (Fig. 5H). This heterogeneity highlights the possible route for DS cell migration into the inward feather follicle (Fig. 7C). On the other hand, co-staining of LRDCs and *NCAM* by RNAscope (Fig. S5) reveals that higher *NCAM* expression levels in the near resting-phase PP may facilitate LRDC accumulation in the PP close to the DP. Future studies will further characterize the function of these molecular markers.

Cyclic regeneration of the dermal components also enables the reassembly of the dermal niche for the next feather cycle. This provides a unique opportunity to alter the dermal niche depending on the age, sex or seasonal differences to produce different appendage phenotypes through a metamorphosis at the organ level (Chuong et al., 2013). When epithelial stem cells are activated, their cell lineage responds to local cues that direct them toward skin-specific fates to season-specific, region-specific or sex-specific forms at different life stages (Chuong et al., 2012; Widelitz et al., 2019). The source of these modulation cues can arise outside of the body (mega-environmental factors; i.e. temperature or photoperiod), systemically within the body (macro-environmental factors; i.e. hormones, neuronal activity) or locally within the skin (micro-environmental factors; i.e. growth factors, signaling molecules, adhesion molecules). Thus the cyclic regeneration of dermal niches provides temporospatial flexibility and an advantageous platform for feather evolution in the context of Evo-Devo (Chen et al., 2015; Xu et al., 2014).

MATERIALS AND METHODS

Ethics statement

All the animals used in this study were processed following an approved protocol of the Institutional Animal Care and Use Committees of the University of Southern California (USC; Los Angeles, CA, USA).

Chickens

White leghorn chickens were hatched from pathogen-free fertilized eggs (SPAFAS, Preston, CT, USA). Chickens were raised at 22°C with 12-h cycles of light and darkness. Six-month to 1-year-old male chickens were used in this study.

TA cells labeling

For TA cell pulse labeling, adult chickens were injected with BrdU (Sigma-Aldrich, 2 mg/kg) and feathers were collected after 2 h. For TA cell long-term BrdU labeling, BrdU was added to the drinking water (2 mg/kg) daily for 1 week. For TA cell double-labeling, IdU (Sigma-Aldrich, 2 mg/kg) was injected. After 22 h, CldU (Sigma-Aldrich, 2 mg/kg) was injected and feather follicles were collected at 24 h. To quantify the percentage of CldU and IdU cells in pPP and cPP, a line was drawn to separate pPP and cPP (Fig. 2I). Although there is no anatomical boundary between pPP and cPP, the cell density and arrangement were different (Fig. 1A'; Fig. S1). Molecular expression further defined pPP (Fig. 1C-K). Based on these, 100 µm was estimated and used to mark the boundary between the pPP and cPP (Fig. 2I) for quantification ($n=5$ feather follicles).

Label-retaining cells

To label slow-cycling putative stem cells (LRCs), 40 resting-phase contour feathers in the central back were plucked. After regenerating for 1 week, BrdU was added to the drinking water (2 mg/kg) daily for 1 week. Feathers were collected at 0, 2, 4 and 7 weeks after the labeling. Five feather follicles were collected at each time point.

To study the LRDCs during regeneration, a similar strategy as above was implemented, using IdU to label the LRDCs. Resting-phase feathers were plucked. After 2 days, CldU (2 mg/kg) was injected and feather follicles were collected 2 h later. This strategy allowed us to observe both LRDCs and TA cells in the 2-day regenerated feather blastema.

Statistical analysis

In Figs 2J, 3G, 4D, 5E and 6I, data are mean±s.d. All comparisons were made by applying a paired two-tailed Student's *t*-test.

Dermal cell lineage tracing

For early growth-phase DP DiI labeling, the follicle sheath was opened to the base of the feather follicle with fine scissors and 0.2 µl DiI solution (Thermo Fisher Scientific, C7001) was injected into the dorsal DP. Three feather follicles were collected immediately after DiI injection and five feather follicles were collected after 5 days. Feather follicles were embedded in OCT compound (Tissue-Tek, 4583) and frozen on dry ice before sectioning.

For resting-phase DP DiI labeling, we plucked the resting-phase feather and opened the follicle wall. DiI was injected into the dorsal aDP. Three resting-phase DP were collected immediately after DiI injection. After 5 days, five feather follicles were dissected.

For DS labeling with DiI, the early growth-phase follicle sheath was opened to the base of the feather follicle and 0.2 µl DiI solution was injected into the DS. Three feather follicles were collected immediately after DiI labeling and four feather follicles were collected after 24 h.

Table 2. List of RNA-seq samples

	Developmental stage	Number of samples
Different dermal components		
Dermal papilla	Early growth	3
Dermal sheath	Early growth	3
Peripheral pulp	Early growth	3
Central pulp	Early growth	3
Pulp at different developmental stages		
Full pulp	Early growth	2
Full pulp	Late growth	2
Full pulp	Near resting	2
Apical DP	Resting	3

For DS labeling with the Tol2 system, pT2AL200R175-CAGGS-H2BGFP/pCAGGS-T2TP plasmids were prepared at 2 µg/µl, mixed with 10% fast green and then 0.2 µl mixed plasmid was injected into the DS. After adding 100 µl PBS to cover the injection site, electroporation (three pulses of 15v/50 ms) was performed (BTX ECM 830). Samples were collected after 48 h and frozen sections were prepared.

Paraffin section and immunostaining

Feather follicles were fixed in 4% paraformaldehyde at 4°C overnight and 7 µm longitudinal paraffin sections were prepared according to standard procedures (Yue et al., 2005). Immunostaining was followed by procedures previously described by Jiang et al. (1998). We used the following antibodies: Col1 (Abcam, ab34710, 1:200), COL2A1 (Developmental Studies Hybridoma Bank, CIIC1, 1:10), MMP9 (GeneTex, GTX31891, 1:200), SMA (Invitrogen, MA1-37028, 1:200), Sox2 (Abcam, ab97959, 1:200), TGFβ2 (Santa Cruz Biotechnology, SC-90, 1:200), vimentin (Developmental Studies Hybridoma Bank, H5, 1:10). NCAM and TNC were from the Chuong lab (Chuong and Chen, 1991; 1:200).

For BrdU staining, BrdU was detected by mouse anti-BrdU (347580; BD Biosciences, 1:200); anti-mouse AP (Abcam, ab6729, 1:200) was used as secondary antibody; NBT/BCIP solution (Promega) was used to visualize positive staining (blue). For fluorescent BrdU staining, sections were treated with 0.01 M citrate buffer (pH 6.0) by microwaving for 6 min. Alexa Fluor anti-mouse-546 (Invitrogen, A11030, 1:200) was used as a secondary antibody. DAPI was used to visualize the nuclei.

For IdU/CldU double staining, CldU was detected using a rat anti-BrdU antibody (BU 1/75; Ab6326-250; Abcam, 1:200); biotinylated goat anti-mouse IgG (Vector Labs, BA-2000, 1:200) and Streptavidin (Jackson ImmunoResearch, AB_2337238, 1:200) were used as secondary and tertiary antibodies; AEC (Vector Labs) was used to develop the red color. IdU was detected by mouse anti-BrdU (347580; BD, 1:200); anti-mouse AP (Abcam, ab6729, 1:200) was used as a secondary antibody; NBT/BCIP (Promega) was used to visualize positive staining (blue). For fluorescent IdU/CldU staining, sections were treated with 0.01 M citrate buffer (pH 6.0) by microwaving for 6 min. Alexa Fluor anti-mouse-546 (A11030, 1:200) and anti-rat-488 (A11006, 1:200) from Invitrogen were used as secondary antibodies. Stained sections were imaged with an AxioImager (Zeiss). Fluorescent imaging was performed using Keyence BZ-X710 microscope and Leica TCS SP8 confocal microscope.

mRNA *in situ* hybridization

To generate RNA probes, PCR was performed using cDNA from embryonic day 8 chicken skin. PCR primers were: *CDK1* (forward, TATAAA-GGGCGCCACAAAAC; backward, TTGTTGGGTGCCCTAAAGC); *Lgr6* (forward, TGATTACGCCTCCAGAACC; backward, GCTCTAG-GACACGGAGGTTG); *SOSDTC1* (forward, TCTCTCCGCCATTCA-CTTCT; backward, GACAGGCTTTGCTTGTAGAGG). PCR products were inserted to p-drive (Qiagen) to make antisense RNA probes. K15 probes were from Wu et al. (2018). Section *in situ* hybridizations were performed according to procedures described in Wu et al. (2018). Diluted eosin was used for faint counter-staining.

RNAscope

RNAscope was performed using the Multiplex Fluorescent v2 system (ACD; 232100). The standard RNAscope protocol was used according to the manufacturer's instructions. We used the following probes: *FZD8* (1055381-C1), *TNC* (1055441-C2) and *NCAM* (1055371-C3).

To visualize LRDCs and RNAscope data, samples were first recorded using the standard RNAscope procedure. Then, mouse anti-BrdU (347580; BD Biosciences, 1:200) was added. Anti-mouse IgG H&L (HRP) (Abcam, ab6728, 1:200) was used as a secondary antibody; Opal 520 (Akoya Biosciences, SKU FP1487001K) was used to detect the LRCs.

Total RNA isolation and RNA-seq

For different dermal components, early growth-phase contour feathers (regenerated 3 weeks, about 1/3 of final length) in the dorsal tract were used. The feather follicles with intact DP were dissected and only 1 cm of follicle

from the DP was used for further dissection. The follicle sheath beside the DP was dissected. The DP was removed from follicles by pulling with forceps. A cut was made through the side of the feather follicle using fine scissors. When the follicle was opened, the central pulp was removed using forceps. The extra loose pulp in the follicle was peeled off and discarded. The remaining follicle is treated with calcium-magnesium free saline (2×CMF) with 0.1% EDTA on ice for 20 min. Epithelium was then separated from the pPP by peeling with forceps. Thus, the dermal components in a feather follicle were separated into the DP, pPP, cPP and DS. The components from five contour feather follicles were pooled together for further RNA extraction.

Pulp cells were isolated at different developmental stages: early growth-phase (regenerated 3 weeks, about 1/3 of final length), late growth-phase (regenerated 7 weeks, about 2/3 of final length), near resting-phase (regenerated 8 weeks, about full length, but the red color was still visible in the pulp). The resting-phase DPs (regenerated >10 weeks) were also dissected.

Total RNA was isolated using Trizol (Thermo Fisher Scientific, 15596026). The RNA quantities and qualities of each individual were analyzed using a NanoDrop (Thermo Fisher Scientific) and BioAnalyzer II (Agilent Technologies). We used 1 µg of total RNA from each sample to construct an RNA-seq library using TruSeq RNA sample preparation v2 kit (Illumina). Sequencing (50 cycles single read) was performed using Hi-seq 2000 at the USC Epigenome Center. The RNA-seq samples are listed in Table 2.

Read count normalization and DEG identification

The read counts and transcripts per million (TPM) values for each gene were obtained from the mapping files using StringTie (Pertea et al., 2015, 2016) using default parameters and the genome annotation file. Genes with mean TPM value across libraries higher than 1 were defined as the expressed genes (Tables S5, S6). Read counts among the libraries were normalized and DEGs were calculated using DESeq2 (Love et al., 2014). In Fig. 4, samples were from homogeneous tissues, so we applied relatively relaxed thresholds for DEG identification. The expressed genes were defined as DEGs when their log₂ fold change > 2 and *q*-value < 0.01 between the comparisons (Table S1). The comparisons were performed between consecutive points of pulp regeneration. In Fig. 5, samples were from relatively heterogeneous tissues, so we applied relatively stringent thresholds for DEG identification. In this group, DEGs were from pair-wise comparisons between the libraries in criteria of log₂ fold change > 3, and *q*-value < 0.001 (Table S3).

Gene clustering and heatmap construction

DEGs from Figs S4 or S5 were merged and their normalized log₂-transformed values were calculated by DESeq2 and used as the input for the following analysis. The hierarchical clusters and heatmaps were generated from the merged DEGs by the R package ‘pheatmap’ (Raivo Kolde, 2019). Clustering information for Figs S4 and S5 are shown in Tables S2 and S4, respectively. In Fig. 5, the marker genes in each tissue type were defined as the genes exclusively upregulated in one tissue type. Clusters 2+6, clusters 10+1, cluster 5 and cluster 4 were defined as marker gene clusters of the DP, DS, pPP and cPP, respectively (Table S4).

Acknowledgements

We thank the USC Molecular Genomic Core for conducting next-generation sequencing and the USC Norris Medical Library Bioinformatics Service for consultation. Confocal microscopy was performed by the Cell and Tissue Imaging Core of the USC Research Center for Liver Diseases (National Institutes of Health grant P30 DK048522). We also thank the National Center for High-performance Computing for computer time and facilities. We thank Dr Masafumi Inaba for providing the pT2AL200R175-CAGGS-H2BGFP plasmid.

Competing interests

The authors declare no competing or financial interests.

Author contributions

Conceptualization: P.W., M.L., R.B.W., C.-M.C.; Methodology: P.W., T.-X.J., M.L., C.-K.C., S.-M.H.L., C.-M.C.; Software: C.-K.C.; Validation: S.-M.H.L.; Formal analysis: P.W.; Investigation: P.W., T.-X.J., C.-K.C., S.-M.H.L.; Resources: P.W., T.-X.J.,

R.B.W., C.-M.C.; Data curation: C.-K.C.; Writing - original draft: P.W., M.L., C.-K.C., R.B.W., C.-M.C.; Writing - review & editing: P.W., M.L., R.B.W., C.-M.C.; Supervision: C.-M.C.; Project administration: R.B.W., C.-M.C.; Funding acquisition: C.-M.C.

Funding

National Institute of Arthritis and Musculoskeletal and Skin Diseases (RO1 AR47364, R37 AR60306), C.-M.C., P.W., T.-X.J. and R.B.W. are partially supported by a research contract between China Medical University and University of Southern California (5351285884). M.L. is supported by the National Natural Science Foundation of China (82003384), Fundamental Research Funds for the Central Universities (2020CDJYGS003) and Scientific Research Foundation from Chongqing University (02210011044110). C.-K.C. is supported by the IEGG and Animal Biotechnology Center, National Chung Hsing University, Taiwan, and was supported by Postdoctoral Research Abroad Program, Ministry of Science and Technology, Taiwan (107-2917-I-564-024). S.-M.H.L. is supported by the University of Southern California Craniofacial Biology Ph.D. Program, and a graduate fellowship from the Ministry of National Defense of Taiwan. Deposited in PMC for release after 12 months.

Data availability

The full datasets have been deposited in NCBI Gene Expression Omnibus (GEO) under accession number GSE161220.

Peer review history

The peer review history is available online at <https://journals.biologists.com/dev/article-lookup/doi/10.1242/dev.198671>

References

- Abbasi, S. and Biernaskie, J. (2019). Injury modifies the fate of hair follicle dermal stem cell progeny in a hair cycle-dependent manner. *Exp. Dermatol.* **28**, 419-424. doi:10.1111/exd.13924
- Agabalyan, N. A., Rosin, N. L., Rahmani, W. and Biernaskie, J. (2017). Hair follicle dermal stem cells and skin-derived precursor cells: Exciting tools for endogenous and exogenous therapies. *Exp. Dermatol.* **26**, 505-509. doi:10.1111/exd.13359
- Assis-Ribas, T., Forni, M. F., Winnischer, S. M. B., Sogayar, M. C. and Trombetta-Lima, M. (2018). Extracellular matrix dynamics during mesenchymal stem cells differentiation. *Dev. Biol.* **437**, 63-74. doi:10.1016/j.ydbio.2018.03.002
- Biernaskie, J. (2010). Human hair follicles: “bulging” with neural crest-like stem cells. *J. Invest. Dermatol.* **130**, 1202-1204. doi:10.1038/jid.2009.449
- Brown, C., McKee, C., Bakshi, S., Walker, K., Hakman, E., Halassy, S., Svinarich, D., Dodds, R., Govind, C. K. and Chaudhry, G. R. (2019). Mesenchymal stem cells: cell therapy and regeneration potential. *J. Tissue Eng. Regen. Med.* **13**, 1738-1755. doi:10.1002/term.2914
- Chang, C.-H., Yu, M., Wu, P., Jiang, T.-X., Yu, H.-S., Widelitz, R. B. and Chuong, C.-M. (2004). Sculpting skin appendages out of epidermal layers via temporally and spatially regulated apoptotic events. *J. Invest. Dermatol.* **122**, 1348-1355. doi:10.1111/j.0022-202X.2004.22611.x
- Chang, W.-L., Wu, H., Chiu, Y.-K., Wang, S., Jiang, T.-X., Luo, Z.-L., Lin, Y.-C., Li, A., Hsu, J.-T., Huang, H.-L. et al. (2019). The making of a flight feather: bio-architectural principles and adaptation. *Cell* **179**, 1409-1423.e17. doi:10.1016/j.cell.2019.11.008
- Chen, C.-F., Foley, J., Tang, P.-C., Li, A., Jiang, T. X., Wu, P., Widelitz, R. B. and Chuong, C. M. (2015). Development, regeneration, and evolution of feathers. *Annu. Rev. Anim. Biosci.* **3**, 169-195. doi:10.1146/annurev-animal-022513-114127
- Chi, W. Y., Enshell-Seiffers, D. and Morgan, B. A. (2010). De novo production of dermal papilla cells during the anagen phase of the hair cycle. *J. Invest. Dermatol.* **130**, 2664-2666. doi:10.1038/jid.2010.176
- Chi, W., Wu, E. and Morgan, B. A. (2013). Dermal papilla cell number specifies hair size, shape and cycling and its reduction causes follicular decline. *Development* **140**, 1676-1683. doi:10.1242/dev.090662
- Chu, Q., Cai, L., Fu, Y., Chen, X., Yan, Z., Lin, X., Zhou, G., Han, H., Widelitz, R. B., Chuong, C. et al. (2014). Dkk2/Frzb in the dermal papillae regulates feather regeneration. *Dev. Biol.* **387**, 167-178. doi:10.1016/j.ydbio.2014.01.010
- Chuong, C.-M. and Chen, H.-M. (1991). Enhanced expression of N-CAM and tenascin during wound healing. *Am. J. Pathol.* **138**, 427-440.
- Chuong, C.-M., Wu, P., Zhang, F.-C., Xu, X., Yu, M., Widelitz, R. B., Jiang, T.-X. and Hou, L. (2003). Adaptation to the sky: Defining the feather with integument fossils from mesozoic China and experimental evidence from molecular laboratories. *J. Exp. Zool. B Mol. Dev. Evol.* **298**, 42-56. doi:10.1002/jez.b.25
- Chuong, C.-M., Randall, V. A., Widelitz, R. B., Wu, P. and Jiang, T.-X. (2012). Physiological regeneration of skin appendages and implications for regenerative medicine. *Physiology (Bethesda)* **27**, 61-72. doi:10.1152/physiol.00028.2011
- Chuong, C.-M., Yeh, C.-Y., Jiang, T.-X. and Widelitz, R. (2013). Module-based complexity formation: periodic patterning in feathers and hairs. *Wiley Interdiscip. Rev. Dev. Biol.* **2**, 97-112. doi:10.1002/wdev.74

- Elliott, K., Stephenson, T. J. and Messenger, A. G.** (1999). Differences in hair follicle dermal papilla volume are due to extracellular matrix volume and cell number: implications for the control of hair follicle size and androgen responses. *J. Invest. Dermatol.* **113**, 873-877. doi:10.1046/j.1523-1747.1999.00797.x
- Feutz, A.-C., Barrandon, Y. and Monard, D.** (2008). Control of thrombin signaling through PI3K is a mechanism underlying plasticity between hair follicle dermal sheath and papilla cells. *J. Cell Sci.* **121**, 1435-1443. doi:10.1242/jcs.018689
- Fuchs, E.** (2018). Skin stem cells in silence, action, and cancer. *Stem Cell Rep.* **10**, 1432-1438. doi:10.1016/j.stemcr.2018.04.008
- Gonzales, K. A. U. and Fuchs, E.** (2017). Skin and its regenerative powers: an alliance between stem cells and their niche. *Dev. Cell* **43**, 387-401. doi:10.1016/j.devcel.2017.10.001
- González, R., Moffatt, G., Hagner, A., Sinha, S., Shin, W., Rahmani, W., Chojnacki, A. and Biernaskie, J.** (2017). Platelet-derived growth factor signaling modulates adult hair follicle dermal stem cell maintenance and self-renewal. *NPJ Regen. Med.* **2**, 11. doi:10.1038/s41536-017-0013-4
- Gupta, K., Levinsohn, J., Linderman, G., Chen, D., Sun, T. Y., Dong, D., Taketo, M. M., Bosenberg, M., Kluger, Y., Choate, K. et al.** (2019). Single-cell analysis reveals a hair follicle dermal niche molecular differentiation trajectory that begins prior to morphogenesis. *Dev. Cell* **48**, 17-31.e6. doi:10.1016/j.devcel.2018.11.032
- Horne, K. A. and Jahoda, C. A.** (1992). Restoration of hair growth by surgical implantation of follicular dermal sheath. *Development* **116**, 563-571. doi:10.1242/dev.116.3.563
- Jiang, T.-X., Stott, S., Widelitz, R. B. and Chuong, C.-M.** (1998). Current methods in the study of avian skin appendages. In *Molecular Basis of Epithelial Appendage Morphogenesis* (ed. C. M. Chuong), pp. 395-408. Austin, TX: Landes Bioscience.
- Knapp, D. and Tanaka, E. M.** (2012). Regeneration and reprogramming. *Curr. Opin. Genet. Dev.* **22**, 485-493. doi:10.1016/j.gde.2012.09.006
- Lai, Y. C. and Chuong, C.-M.** (2016). The "tao" of integuments. *Science* **354**, 1533-1534. doi:10.1126/science.aal4572
- Li, J., Jiang, T.-X., Hughes, M. W., Wu, P., Yu, J., Widelitz, R. B., Fan, G. and Chuong, C.-M.** (2012). Progressive alopecia reveals decreasing stem cell activation probability during aging of mice with epidermal deletion of DNA methyltransferase 1. *J. Invest. Dermatol.* **132**, 2681-2690. doi:10.1038/jid.2012.206
- Li, A., Figueroa, S., Jiang, T.-X., Wu, P., Widelitz, R., Nie, Q. and Chuong, C.-M.** (2017). Diverse feather shape evolution enabled by coupling anisotropic signalling modules with self-organizing branching programme. *Nat. Commun.* **8**, ncomms14139. doi:10.1038/ncomms14139
- Lillie, F. R. and Wang, H.** (1941). Physiology of development of the feather V. Experimental morphogenesis. *Physiol. Zool.* **14**, 103-135.
- Lillie, F. R.** (1940). Physiology of development of the feather. III growth of the mesodermal constituents and blood circulation in the pulp. *Physiol. Zool.* **13**, 143-176.
- Lin, S. J., Foley, J., Jiang, T. X., Yeh, C. Y., Wu, P., Foley, A., Yen, C. M., Huang, Y. C., Cheng, H. C., Chen, C. F. et al.** (2013). Topology of feather melanocyte progenitor niche allows complex pigment patterns to emerge. *Science* **340**, 1442-1445. doi:10.1126/science.1230374
- Love, M. I., Huber, W. and Anders, S.** (2014). Moderated estimation of fold change and dispersion for RNA-seq data with DESeq2. *Genome Biol.* **15**, 550. doi:10.1186/s13059-014-0550-8
- Lucas, A. M. and Stettenheim, P. R.** (1972). *Avian Anatomy. Integument*. Agriculture Handbook 362. Washington, DC: U.S. Department of Agriculture.
- Maderson, P. F. A., Hillenius, W. J., Hiller, U. and Dove, C. C.** (2009). Towards a comprehensive model of feather regeneration. *J. Morphol.* **270**, 1166-1208. doi:10.1002/jmor.10747
- McElwee, K. J., Kissling, S., Wenzel, E., Huth, A. and Hoffmann, R.** (2003). Cultured peribulbar dermal sheath cells can induce hair follicle development and contribute to the dermal sheath and dermal papilla. *J. Invest. Dermatol.* **121**, 1267-1275. doi:10.1111/j.1523-1747.2003.12568.x
- Morgan, B. A.** (2014). The dermal papilla: an instructive niche for epithelial stem and progenitor cells in development and regeneration of the hair follicle. *Cold Spring Harb. Perspect. Med.* **4**, a015180. doi:10.1101/cshperspect.a015180
- Nombela-Arrieta, C., Ritz, J. and Silberstein, L. E.** (2011). The elusive nature and function of mesenchymal stem cells. *Nat. Rev. Mol. Cell Biol.* **12**, 126-131. doi:10.1038/nrm3049
- Perteau, M., Perteau, G. M., Antonescu, C. M., Chang, T.-C., Mendell, J. T. and Salzberg, S. L.** (2015). StringTie enables improved reconstruction of a transcriptome from RNA-seq reads. *Nat. Biotechnol.* **33**, 290-295. doi:10.1038/nbt.3122
- Perteau, M., Kim, D., Perteau, G. M., Leek, J. T. and Salzberg, S. L.** (2016). Transcript-level expression analysis of RNA-seq experiments with HISAT, StringTie and Ballgown. *Nat. Protoc.* **11**, 1650-1667. doi:10.1038/nprot.2016.095
- Rahmani, W., Abbasi, S., Hagner, A., Raharjo, E., Kumar, R., Hotta, A., Magness, S., Metzger, D. and Biernaskie, J.** (2014). Hair follicle dermal stem cells regenerate the dermal sheath, repopulate the dermal papilla, and modulate hair type. *Dev. Cell* **31**, 543-558. doi:10.1016/j.devcel.2014.10.022
- Raivo Kolde** (2019). heatmap: Pretty Heatmaps. *R Package Version 1.0.12*.
- Shin, W., Rosin, N. L., Sparks, H., Sinha, S., Rahmani, W., Sharma, N., Workentine, M., Abbasi, S., Labit, E., Stratton, J. A. et al.** (2020). Dysfunction of hair follicle mesenchymal progenitors contributes to age-associated hair loss. *Dev. Cell* **53**, 185-198.e7. doi:10.1016/j.devcel.2020.03.019
- Tobin, D. J., Gunin, A., Magerl, M., Handjiski, B. and Paus, R.** (2003). Plasticity and cytokinetic dynamics of the hair follicle mesenchyme: implications for hair growth control. *J. Invest. Dermatol.* **120**, 895-904. doi:10.1046/j.1523-1747.2003.12237.x
- Widelitz, R. B., Lin, G.-W., Lai, Y.-C., Mayer, J. A., Tang, P.-C., Cheng, H.-C., Jiang, T.-X., Chen, C.-F. and Chuong, C.-M.** (2019). Morpho-regulation in diverse chicken feather formation: Integrating branching modules and sex hormone-dependent morpho-regulatory modules. *Dev. Growth Differ.* **61**, 124-138. doi:10.1111/dgd.12584
- Wu, P., Lai, Y.-C., Widelitz, R. and Chuong, C.-M.** (2018). Comprehensive molecular and cellular studies suggest avian scutate scales are secondarily derived from feathers, and more distant from reptilian scales. *Sci. Rep.* **8**, 16766. doi:10.1038/s41598-018-35176-y
- Xu, X., Zhou, Z., Dudley, R., Mackem, S., Chuong, C.-M., Erickson, G. M. and Varricchio, D. J.** (2014). An integrative approach to understanding bird origins. *Science* **346**, 1253293. doi:10.1126/science.1253293
- Yang, H., Adam, R. C., Ge, Y., Hua, Z. L. and Fuchs, E.** (2017). Epithelial-mesenchymal micro-niches govern stem cell lineage choices. *Cell* **169**, 483-496.e13. doi:10.1016/j.cell.2017.03.038
- Yu, M., Yue, Z., Wu, P., Wu, D.-Y., Mayer, J.-A., Medina, M., Widelitz, R. B., Jiang, T.-X. and Chuong, C.-M.** (2004). The biology of feather follicles. *Int. J. Dev. Biol.* **48**, 181-191. doi:10.1387/ijdb.15272383
- Yue, Z., Jiang, T.-X., Widelitz, R. B. and Chuong, C.-M.** (2005). Mapping stem cell activities in the feather follicle. *Nature* **438**, 1026-1029. doi:10.1038/nature04222
- Yue, Z., Jiang, T.-X., Widelitz, R. B. and Chuong, C.-M.** (2006). Wnt3a gradient converts radial to bilateral feather symmetry via topological arrangement of epithelia. *Proc. Natl. Acad. Sci. USA* **103**, 951-955. doi:10.1073/pnas.0506894103
- Yue, Z., Jiang, T. X., Wu, P., Widelitz, R. B. and Chuong, C. M.** (2012). Sprouty/FGF signaling regulates the proximal-distal feather morphology and the size of dermal papillae. *Dev. Biol.* **372**, 45-54. doi:10.1016/j.ydbio.2012.09.004